Cellular Microbiology (2014) **16**(10), 1549–1564
doi:10.1111/cmi.12311
First published online 13 June 2014

# Cell-to-cell transfer of *Leishmania amazonensis* amastigotes is mediated by immunomodulatory LAMP-rich parasitophorous extrusions

**Fernando Real,[1]* Pilar Tavares Veras Florentino,[1] Luiza Campos Reis,[2] Eduardo M. Ramos-Sanchez,[2] Patricia Sampaio Tavares Veras,[3] Hiro Goto[2,4] and Renato Arruda Mortara[1]**

[1]*Departamento de Microbiologia, Imunologia e Parasitologia, Escola Paulista de Medicina, Universidade Federal de São Paulo (EPM-UNIFESP), São Paulo, Brasil.*

[2]*Laboratório de Soroepidemiologia e Imunobiologia, Instituto de Medicina Tropical, Universidade de São Paulo, São Paulo, Brasil.*

[3]*Instituto Nacional de Ciência e Tecnologia em Doenças Tropicais (INCT – DT), Fundação Oswaldo Cruz (FIOCRUZ), Bahia, Brasil.*

[4]*Departamento de Medicina Preventiva, Faculdade de Medicina, Universidade de São Paulo, São Paulo, Brasil.*

## Summary

**The last step of *Leishmania* intracellular life cycle is the egress of amastigotes from the host cell and their uptake by adjacent cells. Using multi-dimensional live imaging of long-term-infected macrophage cultures we observed that *Leishmania amazonensis* amastigotes were transferred from cell to cell when the donor host macrophage delivers warning signs of imminent apoptosis. They were extruded from the macrophage within zeiotic structures (membrane blebs, an apoptotic feature) rich in phagolysosomal membrane components. The extrusions containing amastigotes were selectively internalized by vicinal macrophages and the rescued amastigotes remain viable in recipient macrophages. Host cell apoptosis induced by micro-irradiation of infected macrophage nuclei promoted amastigotes extrusion, which were rescued by non-irradiated vicinal macrophages. Using amastigotes isolated from LAMP1/LAMP2 knockout fibroblasts, we observed that the presence of these lysosomal components on amastigotes increases interleukin 10 production. Enclosed within host cell membranes, amastigotes can be transferred from cell to cell without full exposure to the extracellular milieu, what represents an important strategy developed by the parasite to evade host immune system.**

Received 22 July, 2013; revised 29 April, 2014; accepted 8 May, 2014. *For correspondence. E-mail: fernando.real@unifesp.br; Tel. (+55) 11 5571 1095 ext. 32; Fax +55 11 5576-4848.

## Introduction

*Leishmania* infections, which affect around 2 million people globally each year (WHO, 2010), are transmitted to vertebrate hosts by infected insect vectors. In the infected mammalian host, *Leishmania* are predominantly sheltered within macrophage-like cells. Thus, the mechanism involved in their macrophage-to-macrophage transfer in the cutaneous or visceral lesions is an important area of study. However, the steps of the intracellular life cycle in mammalian hosts that involve the obligatory egress of *Leishmania* amastigote forms from host cells in order to the spread to new host cells and other tissues (tropism) and organisms are likely the least known aspect of the biology of this parasitic protozoan. A search of the early literature revealed that authors emphasized a 'lytic' cycle for this parasite, mainly based on histopathological observations fragmented in space and time (Theodorides, 1997; Dedet, 2007; Florentino *et al.*, 2014). The preferential, almost exclusive, presence of oval-shaped parasites inside macrophages was the most puzzling aspect of leishmaniasis for the first histopathologists who studied the organism (Wright, 1903; Christophers, 1904), highlighting the uniqueness of *Leishmania* cell infection and supporting a concept of a specialized parasite, with a limited repertoire of cells able to host them. For decades, leishmaniasis was considered a disease almost exclusively of the host macrophage system (Meleney, 1925; Heyneman, 1971).

The first attempt to unveil *Leishmania* egress from infected host cells appears to be one study published in 1980, in which parasites were observed lying free on the edge of cellular infiltration as product of host cell lysis (Ridley, 1980). Macrophage lysis or the presence of extracellular amastigotes were not observed in infected tissues presenting decreased inflammatory response.

These findings suggested that amastigote release is a consequence of the cytolytic environment modulated by host immune response and may be not actively promoted by parasites. The egress of amastigotes was revisited in the literature in the late 1990s (Rittig *et al*., 1998; Rittig and Bogdan, 2000). The long-term observation of cells hosting *Leishmania major* by live microscopy revealed that 'after several uneventful days, small vacuoles suddenly accumulated asymmetrically at the periphery of the infected phagocytes' where amastigotes were 'constantly released over a period of several hours, leaving the somewhat shrivelled remnants of their host cells'. An alternative view of parasite egress was proposed, in which amastigotes would be released in a synchronized fashion, through an exocytosis-like process; it assumes that *Leishmania* egress does not necessarily require host cell lysis by an amastigote multiplication burst.

In this report, using live imaging microscopic evidence, we revisited and further investigated the previously described amastigote exit from host cells (Rittig *et al*., 1998; Rittig and Bogdan, 2000); we propose that host cell exit of *Leishmania* takes place from damaged host cells, in a process mediated by parasitophorous extrusions. These structures fully or partially surrounded amastigotes and were rich in host phagolysosomal components, especially lysosome-associated membrane proteins (LAMPs), which stimulated the production of anti-inflammatory cytokines.

## Results

### *Amastigotes are transferred from cell to cell during host cell death*

The continuous live cell recordings of bone marrow-derived macrophages (BMDMØ) infected with *Leishmania amazonensis*-DsRed2 amastigotes for the first 48 h of infection *in vitro* did not provide evidence of cell-to-cell transference of the intracellular form of the parasite (Real and Mortara, 2012). We decided to examine *L. amazonensis*-DsRed2 cell-to-cell transfer in long-term cultivated BMDMØ (> 4 days) considering that (i) these cells can be cultivated *in vitro* for several days, with minimum multiplication (Rabinovitch and De Stefano, 1973; Eischen *et al*., 1991), (ii) some host macrophages will display a controlled cell death programme in prolonged cultivation, and (iii) an exhausted host cell population, identified by controlled cell death markers, would drive amastigote exit and transference between cells.

First, the pro-apoptotic Bax gene expression assessed by qPCR as a marker of ongoing apoptotic process in macrophage cultures was studied to define the time window when amastigote cell-to-cell transfers would potentially occur. The expression of Bax is increased after 4 and 10 days of cultivation in infected and non-infected cultures (Fig. 1A). Second, we co-incubated BMDMØ that had been infected *in vitro* for 20 days with *L. amazonensis*-DsRed2 with fresh uninfected RAW 264.7 macrophage-like cells. RAW cells were observed to selectively take-up, or rescue, extruded amastigotes from damaged infected macrophages (Fig. 1B, Video S1A). Recipient RAW macrophages interact with donor BMDMØ in the imminence of apoptosis process; the long-term infected BMDMØ shrunk and became zeiotic, forming membrane blebs (Fig. 1B, arrowheads). Amastigotes rescued by adjacent BMDMØ or by fresh RAW cells survive in the new environment and develop spacious PVs in the recipient host cytoplasm. Recipient RAW cells or BMDMØ usually migrate towards donor host macrophages, extending their pseudopodia to and selectively reaching extruded amastigotes (Video 1A at time point 1d05:45, and Fig. 1C). Amastigote transfers between non-affected viable cells were not observed. Using BMDMØ-GFP infected with *L. amazonensis*-DsRed2, we observed the host cell and spacious PV shrinkage, with concomitant relocation of some amastigotes into the zeiotic structures (Fig. 1D arrowheads and Video S1B).

Our observation of BMDMØ that had been infected *in vitro* for 15 days with *L. amazonensis*-DsRed2 followed by additional 3 days of live microscopy revealed several cases in which amastigotes were rescued from affected macrophage (donor cells) by vicinal, recipient cells of the same lineage (Fig. 2A, Video S2). Transfers occurred in the first hours of host cell alteration and involve the mobilization of recipient cells towards donor cells. These events were quantified in live cell recordings, in parallel with automatic cell quantification based on Hoechst stain of macrophage nuclei (Fig. 2B, Video S2). Although the numbers of infected and non-infected macrophages decreased at similar rates, the live cell recordings from 15 to 18 days post-infection started with a higher number of cells per field in the infected sample (Fig. 2B, graph). Quantitative PCR for the expression of anti-apoptotic gene mRNAs (IGF-I and Bcl-2) revealed that during long-term cultivation (10 days *in vitro*) infected samples express more anti-apoptotic gene mRNAs than non-infected cultures (Fig. 2C). During the additional 70 h of infection in which macrophage live imaging was recorded, a median of 12 amastigote transfers per field was counted, occurring throughout the entire acquisition period (Fig. 2D).

### *Laser-induced cell death of infected macrophages hasten the amastigote extrusion and transmission*

Considering that amastigotes exit from apoptotic-like macrophages, we investigated whether induction of host

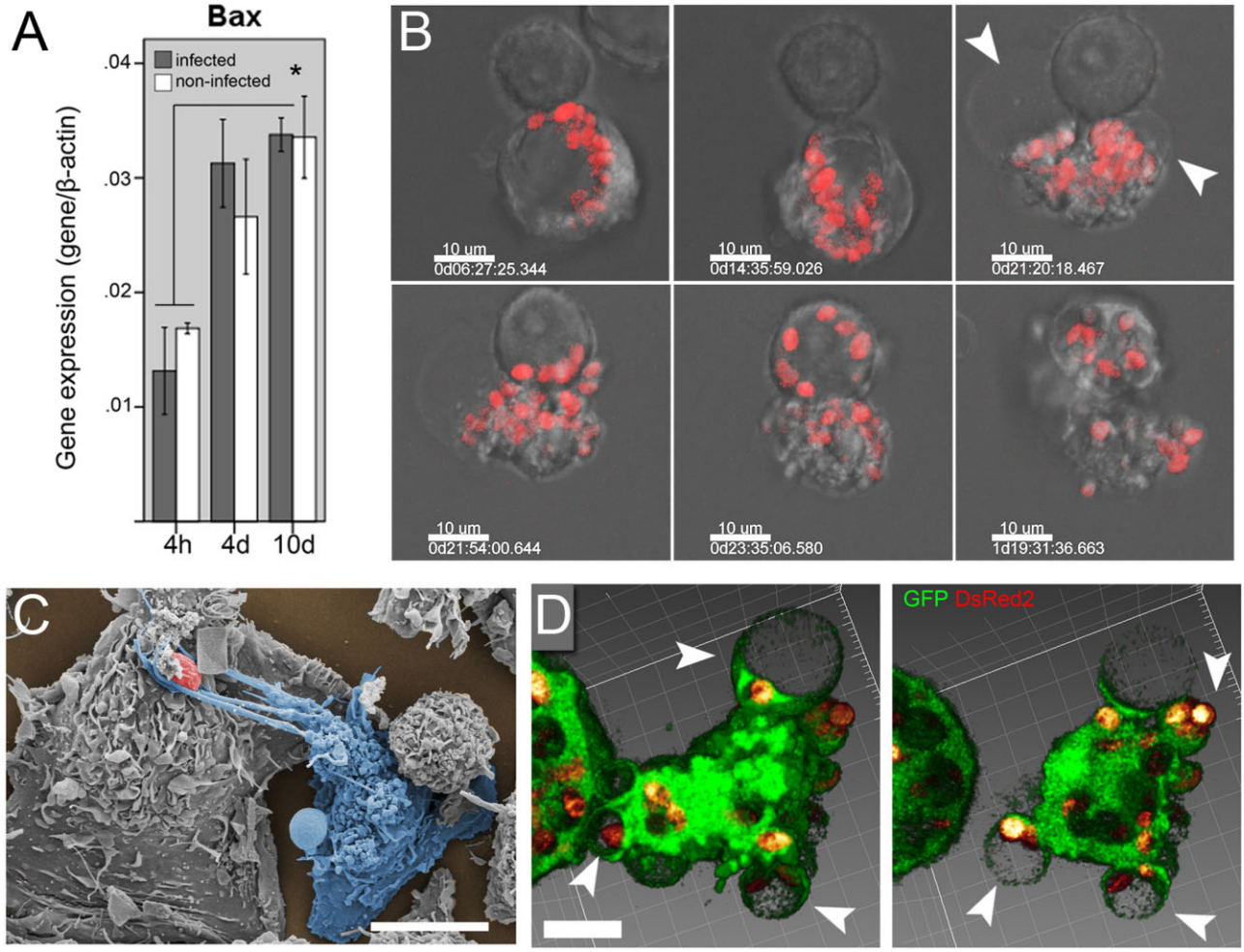


**Fig. 1.** Cell-to-cell transfer of *Leishmania amazonensis* amastigotes occurred after host cell death.
A. Pro-apoptotic Bax gene mRNA expression measured by qPCR in infected or non-infected BMDMØ after 4 h, 4 and 10 days after *L. amazonensis* infection. The data are presented as the relative quantification $2^{-\Delta\Delta Ct}$ against β-actin gene expression. There was an increase in Bax expression after 4 and 10 days, independent of infection. ANOVA, $P < 0.05$.
B. Live cell imaging of BMDMØ infected with *L. amazonensis*-DsRed2 (red) for 30 days *in vitro* and co-cultured with uninfected RAW 264.7 macrophage-like cells. RAW cell interacts with infected BMDMØ and rescue several amastigotes after macrophage collapse. Host cell death presented zeiosis (arrowheads), a typical feature of apoptosis. The time of image acquisition is represented by days:hours:minutes:seconds:milliseconds (d:hh:mm:ss:sss). Image acquisition started after 2 h of RAW cell addition. Bar = 10 μm.
C. Field-emission scanning electron microscopy (FE-SEM) of a BMDMØ culture infected with *L. amazonensis*-DsRed2 for 20 days, showing a macrophage (coloured in blue) interacting with an oval-shaped structure (red) extruded from a vicinal macrophage. This structure presents dimensions compatible with an amastigote. Bar = 10 μm.
D. Amastigotes (red) are extruded from dying BMDMØ-GFP (green) within zeiotic structures (blebs). Images are representative of two z-stacks of the same macrophage and the arrowheads indicate parasite-containing extrusions. Bar = 10 μm. Results are representative of two experiments.

cell apoptosis would trigger *L. amazonensis* extrusion and its rescue by adjacent macrophages. Our challenge was to selectively induce apoptosis in some cells, sparing vicinal macrophages from death in order to allow viable cells to rescue extruded amastigotes. To do so, the nuclei of some infected BMDMØ-GFP in the microscopic field were micro-irradiated by near UV laser (405 nm). A concentrated pulse of UV lasers (351 nm and 364 nm) on the HeLa cell nucleus is known to induce the destruction of these cells via apoptosis (Soustelle *et al.*, 2008).

Figure 3A and Supplementary Video S3 demonstrate that, in the same microscopic field, non-irradiated macrophages were able to rescue amastigotes from apoptotic-like irradiated cells, suggesting that amastigotes benefit from host cell death to spread among other cells. Amastigotes were rescued by adjacent macrophages in 21 out of 31 apoptotic, micro-irradiated BMDMØ (total of 47 micro-irradiated host cells, $n = 3$ experiments). Amastigote transfer started after 6 h post-micro-irradiation. The morphology of macrophage nuclei during

 

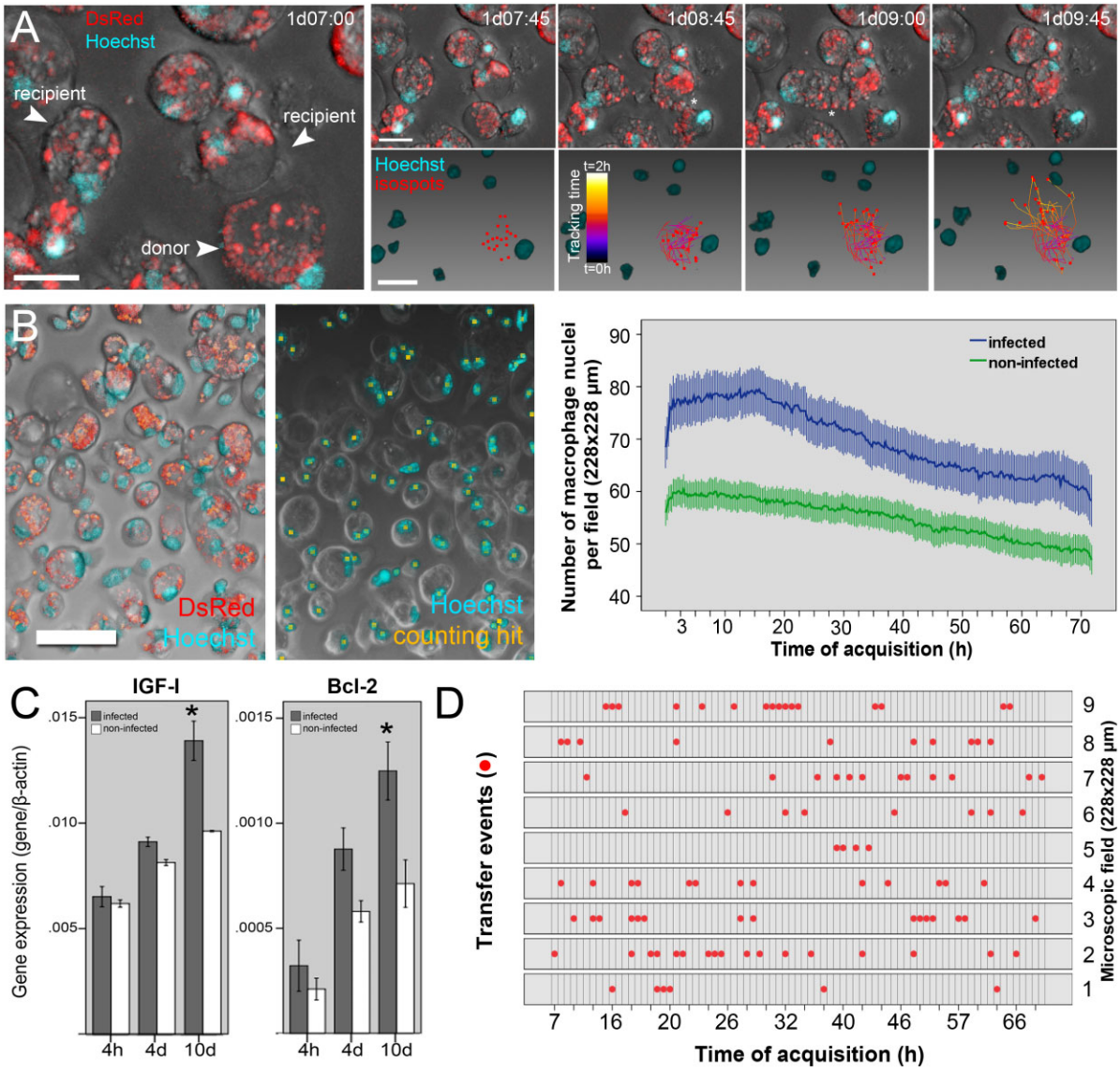


**Fig. 2.** Quantification of amastigote transfer events and host cell numbers during multidimensional acquisition of BMDMØ infected with *L. amazonensis*-DsRed2.

A. Example of *L. amazonensis*-DsRed2 cell-to-cell transfer recorded between BMDMØ infected for 15 days. The image shows the macrophages involved in transfer (arrowheads), classified as donor (a macrophage from which parasites are extruded and transferred after host cell death) and recipient (viable macrophages in the vicinity which rescue extruded parasites from donor). Upper panel: at time point 1d07:45 amastigotes are relocated to a macrophage extrusion; recipient macrophages take up these extruded parasites at time points 1d08:45 and 1d09:00 (asterisks indicate regions of parasite transfers). *L. amazonensis*-DsRed2 in red, Hoechst 33342 staining in cyan channel. Lower panel: amastigotes were tracked during transfer, in an interval of 2 h after amastigote extrusion; parasites displacement in x, y and z dimensions is depicted as tracing lines in each time point. Tracing lines display a colorimetric range, relative to the start (extrusion, t = 0 h, time point 1d07:45, black-blue tracing) and the end of tracking (complete transfer, time point 1d09:45, yellow-white tracing). Macrophage nuclei (Hoechst 33342 staining) in cyan, software-detected amastigotes (isospots) in red squares. Displayed time corresponds to image acquisition elapsed time, after 15 days of infection. Bars = 20 µm.

B. Example of a microscopic field of infected culture showing in the first DIC image merged with red (*L. amazonensis*-DsRed2) and blue (Hoechst 33342) fluorescence channels and in the second image the automated recognition of macrophage nuclei by software analysis (yellow = counting hit), employed to quantify the number of host cells during multidimensional imaging. This automatic quantification was applied to 10 multidimensional images of infected and non-infected cultures, acquired after 15 of infection, for additional 70 h. Right panel (graph): quantified nuclei of infected and non-infected BMDMØ cultures were plotted in the graph, which shows the mean (with standard error) number of macrophage nuclei per microscopic field (40× objective, 228 × 228 µm).

C. Anti-apoptotic genes IGF-I and Bcl-2 mRNA expression measured by qPCR in infected or non-infected BMDMØ after 4 h, 4 and 10 days after *L. amazonensis* infection. The data are presented as the relative quantification $2^{-\Delta\Delta Ct}$ against β-actin gene expression. Infected cell cultures express higher levels of IGF-I and Bcl-2 after 10 days of infection. ANOVA, $P < 0.05$.

D. Quantification of amastigote transfer events (red dots) per microscopic field (40× objective, 228 × 228 µm, $n = 9$). A median of 12 transfers per field was observed in live cell recordings.

 

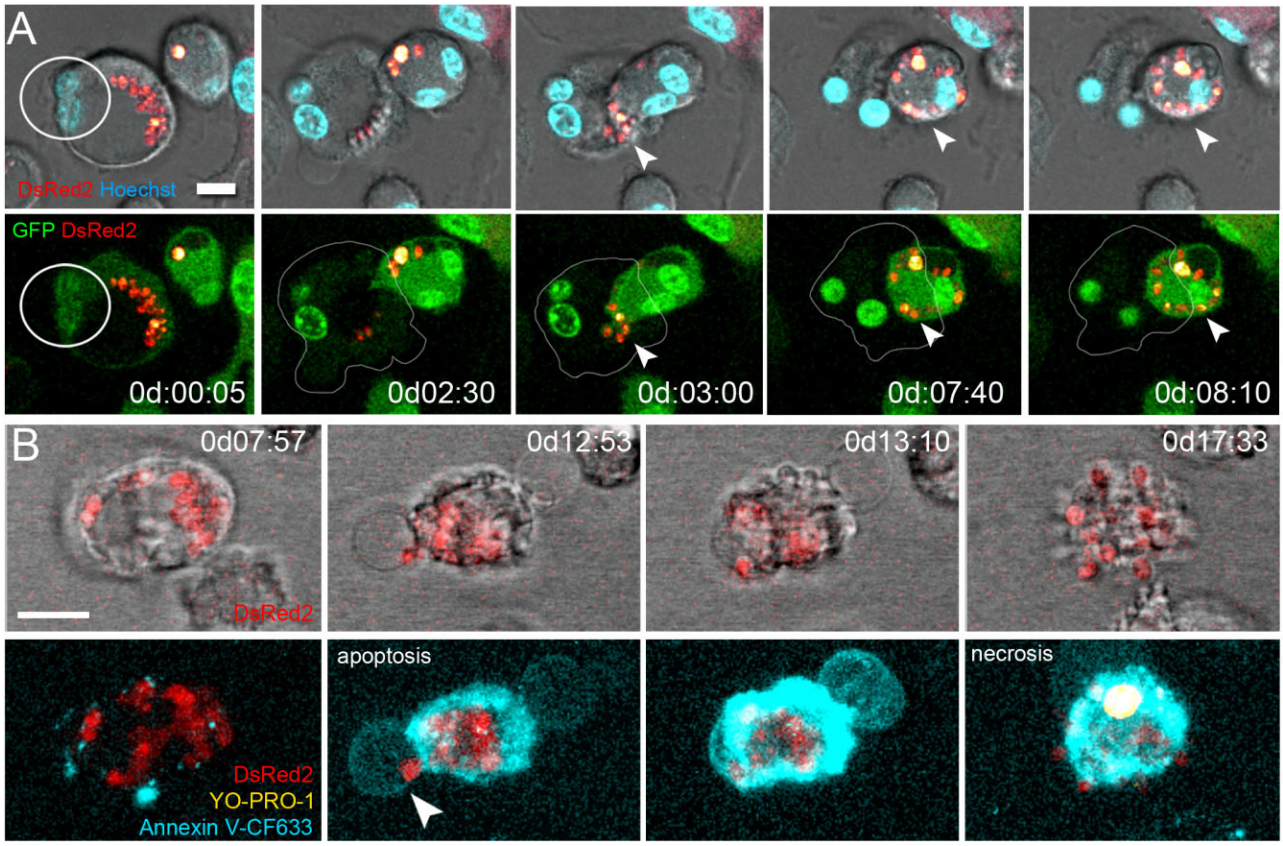


**Fig. 3.** Micro-irradiation of host cell nuclei induced cell death and amastigote transfer.
A. Time-lapse frames of a micro-irradiated BMDMØ-GFP transferring amastigotes (arrowheads) to non-irradiated macrophages. Upper panels: *Leishmania amazonensis*-DsRed2 in red and Hoechst 33342 in cyan, merged with DIC image. Lower panels: green (GFP signal from macrophages) and red channels of the same region, showing GFP leakage of the micro-irradiated cells (contour) during amastigote transfers (arrowhead). The micro-irradiation spot is indicated by a white circle. Image acquisition started after 120 h of infection plus 5 min of micro-irradiation.
B. Multidimensional live imaging of micro-irradiated, 48 h infected BMDMØ in the presence of the phosphatidylserine (PS) probe Annexin V (conjugated to CF633 flurophore, cyan) and the cell membrane-impermeant nucleic probe YO-PRO-1 Iodide (yellow). At time point 0d12:53, during macrophage apoptosis (Annexin V-positive, YO-PRO-1-negative staining), *L. amazonensis*–DsRed2 amastigotes (red) are relocated to zeiotic structures which expose PS (arrowhead); the host cell starts necrosis around 0d14:00 (YO-PRO-1 staining is indicative of loss of membrane integrity). Time of image acquisition is represented by days:hours:minutes (d:hh:mm). Bar = 10 μm.

*L. amazonensis* extrusion was followed in the multidimensional images of Hoechst staining; nuclei shrinkage and condensation of chromatin in the periphery of the nuclei were observed. Additionally, cell shrinkage and zeiosis were also observed, suggesting an apoptosis-like host cell death in the process of amastigote transfer. In experiments employing 48 h infected BMDMØ micro-irradiated in the presence of the fluorescent probes YO-PRO-1 and Annexin V-CF633, we confirmed that micro-irradiation of BMDMØ nuclei induced apoptosis (Annexin-positive/YO-PRO-1-negative staining) then late necrosis (double positive). Figure 3B and Supplementary Video S4 show one case in which an infected BMDMØ, micro-irradiated for 7 min enters apoptosis 12 h post-irradiation and late necrosis 1 h thereafter (Fig. 3B). An extruded, annexin-positive *L. amazonensis*-DsRed2-containing PV is observed during macrophage apoptosis (arrowhead).

Our observation of micro-irradiation-induced amastigote transfers suggests that these events occurred during macrophage GFP leakage (Fig. 3A, white cell contours), evidencing the lack of host cell membrane integrity. To examine if damage to infected macrophage plasma membrane could trigger amastigote transfer, long-term infected BMDMØ-GFP cultures were treated with the bacterial toxin SLO, which is known to form pores on cholesterol-containing membranes (Tweten, 2005). Since the membrane of amastigotes contains ergosterol instead of cholesterol, SLO should not be active on the membrane of the parasites (Fernandes *et al.*, 2011). The quantification of amastigote transfer events by the observation of multidimensional images of infected BMDMØ-GFP treated with SLO revealed an increase in amastigote transfer events when compared with non-treated controls (Supplementary Fig. S1A and B, Video S5A). We also

 

treated infected BMDMØ-GFP with nocodazole, which interferes in microtubule polymerization and has been shown to induce the extrusion of the intracellular bacteria *Chlamydia* (Hybiske and Stephens, 2007). In the majority of macrophages, nocodazole induced the formation of unstable blebs containing amastigotes but neither host cell lysis, as attested by retention of GFP fluorescence in the macrophages, nor cell-to-cell transfer of amastigotes were increased in comparison to untreated control (Supplementary Fig. S1B and C, Video S5B). Classical activation of the macrophages by treatment with IFN-γ and LPS did not trigger amastigote extrusions or transfers.

### *Amastigotes are transferred in association with phagolysosomal components*

Although host cell pores might be involved in amastigote exit, the parasite remains associated with the host membrane during extrusion and transfer. The spacious PVs developed by *L. amazonensis* are rich in phagolysosomal membrane markers such as LAMP and Rab7 proteins, and there is an intimate interaction between amastigotes of this species and the PV membrane (Courret *et al*., 2002; Real and Mortara, 2012). Thus, we investigated if the PV membrane markers LAMP1 and Rab7 would remain associated with the amastigote surface during amastigote extrusion and rescue by adjacent macrophages. In these experiments, we infected LAMP1-GFP- or Rab7-GFP-transfected RAW macrophages with *L. amazonensis*-DsRed2 amastigotes and recorded events of parasite extrusion by multidimensional imaging (Fig. 4A and B, Video S6A–D). We observed the extrusion of amastigotes fully covered by LAMP1 or Rab7 proteins and the transfer of amastigotes that remained associated with (fully or partially covered by) these phagolysosome/PV markers (Fig. 4A, arrowheads). LAMP1 or Rab7 proteins surround extruded amastigotes for minutes, or even hours, after host macrophage zeiosis; then these phagolysosomal markers concentrate on amastigote in a polarized fashion (Fig. 4B, arrowhead). When rescued by adjacent macrophages, amastigotes maintained these phagolysosome markers but not F-actin when actin-RFP-transfected RAW macrophages were investigated under the same experimental conditions (Video S6E).

The ultrastructure of amastigote extrusions confirmed an association between *L. amazonensis* extrusion and host cell membrane. The parasite posterior pole faced the macrophage and was generally associated with macrophage components; the anterior pole faced extracellular milieu when not fully covered by macrophage membrane (Fig. 4C). We observed amastigote extrusion in correlative images of confocal and scanning electron microscopy (Fig. 4D). We found that amastigotes extruded from affected macrophages were fully covered by LAMP1/LAMP2 phagolysosomal proteins, and the amastigote-containing extrusions displayed a smooth surface in contrast to the usually ruffled macrophage surface and with no apparent host membrane pores (Fig. 4D, insets). Amastigotes were wrapped so tightly by host membrane that the extrusions took on the morphology of the parasite (Fig. 4D, extruded parasites are indicated by letters a, b and c). Host macrophages in late necrosis were usually associated with fully exposed amastigotes but some extruded amastigotes still associated with LAMP1 (Supplementary Fig. S2A and B, arrowheads, b). Isotype controls for LAMP1/LAMP2 immunostaining confirmed antibody specificity (Supplementary Fig. S2C and D).

### *Fibroblast-derived amastigotes displaying LAMP on their surfaces stimulate the production of IL-10 by macrophages*

In addition, we examined the importance of PV components on *L. amazonensis* amastigote surface for parasite establishment within recipient macrophages. These host cell components associated with amastigotes could modulate anti-inflammatory immune responses such as IL-10 and TGF-β production, in a fashion similar to the apoptotic mimicry described in *L. amazonensis* infections (Wanderley *et al*., 2006).

To obtain isolated amastigotes associated with PV membranes, parasites were collected after mechanical rupture of host cell cultures or footpad lesion tissues. Host cell remnants, including lysosomal membrane proteins, were previously described to be associated with amastigotes after tissue rupture (Saraiva *et al*., 1983; Winter *et al*., 1994). When isolated from footpad lesions (2 months after inoculum), around 20% of amastigotes remained associated with LAMPs. Incubation of amastigotes under agitation for 2 h decreases this percentage to approximately 4% (Supplementary Fig. S3A).

Amastigotes were also covered by host cell membranes rich in LAMP when isolated from mouse embryonic fibroblasts (MEF) after 48 h of transient infection (Supplementary Fig. S3B and C, Fig. 5A). LAMP immunostaining was associated with amastigote posterior poles as observed by confocal microscopy; scanning electron microscopy (SEM) confirmed the presence of remnants associated with the parasite poles, similar to caps. Amastigotes isolated from LAMP1/LAMP2 double-knockout MEF did not display these lysosomal components on their surfaces but conserved host cell debris on posterior pole (Fig. 5B). The host debris or caps on the amastigote surface were of lysosomal origin, as revealed by the immunostaining of another lysosomal component, lysosomal integral membrane protein-1 (LIMP1).

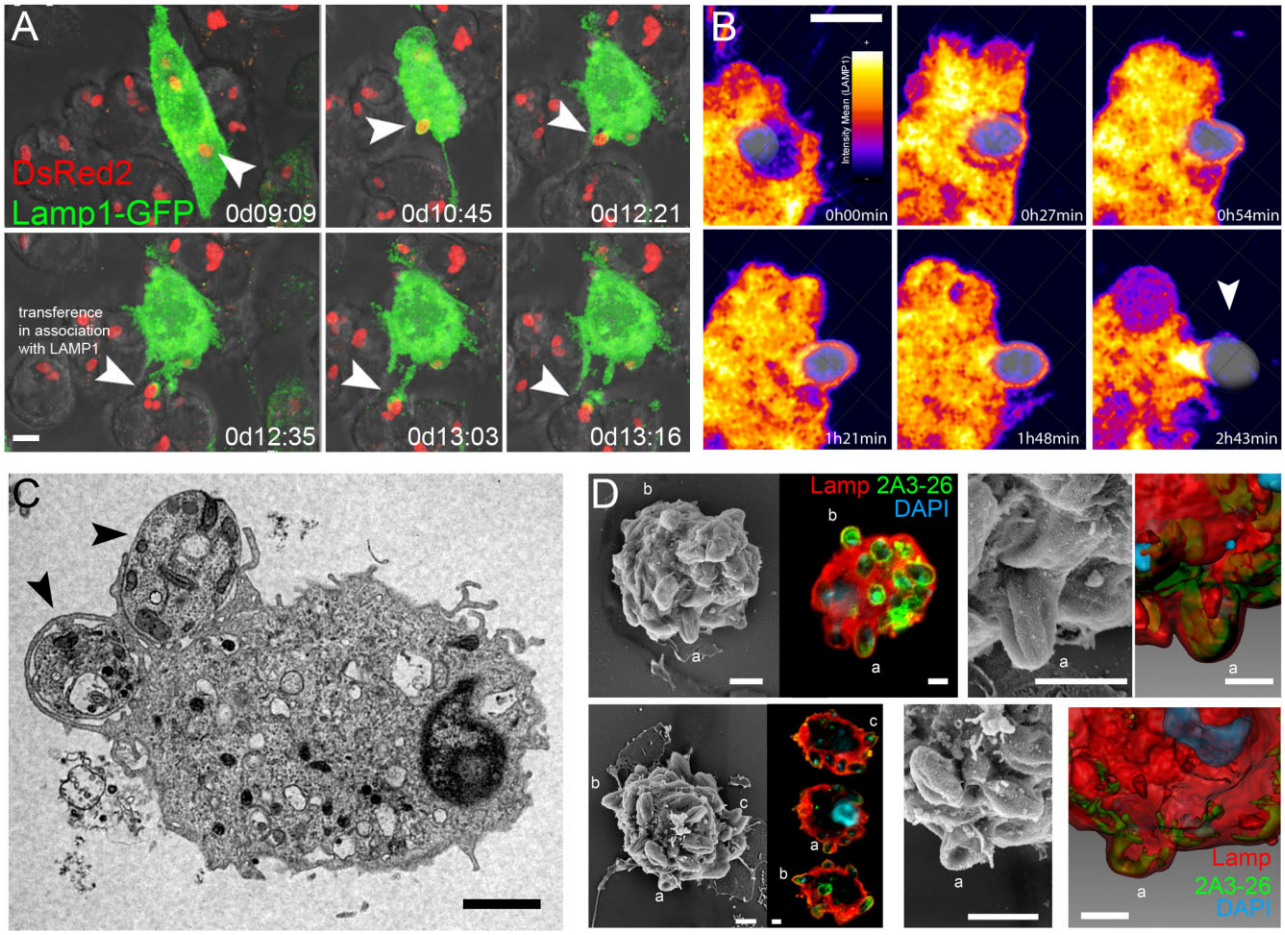


**Fig. 4.** Amastigotes were transferred from cell to cell associated with phagolysosomal components.
A. Multidimensional imaging of RAW 264.7 cells expressing GFP-tagged LAMP1 (in green) and infected with *Leishmania amazonensis*-DsRed2 (red) for 24 h. Arrowheads indicate an extruded amastigote rescued by vicinal macrophage. Time of image acquisition is represented by days:hours:minutes (d:hh:mm). Image acquisition started after 24 h of infection plus 2 min of micro-irradiation. Bars = 10 μm.
B. The temporal sequence of the extrusion event presented in A shows that amastigote is surrounded by LAMP1 (hue-saturation-value filter, colorimetric scale relative to mean fluorescence intensity) during the first hours of extrusion. Later, the extrusion concentrates LAMP1 on an amastigote pole (arrowhead). Relative time of extrusion is represented by hours:minutes (h:mm). Extruded amastigote is indicated by an isosurface (grey) constructed by imaging software, based on DsRed2 signal. Bar = 5 μm.
C. TEM of two amastigotes (arrowheads) extruded from an apoptotic macrophage. The host cell presents apoptotic features such as shrinkage and peripheral chromatin condensation in a deformed nucleus. Amastigotes are fully (left arrowhead) or partially (right arrowhead) exposed to extracellular milieu. Bar = 2 μm.
D. Correlative imaging of infected macrophages extruding amastigotes. The image presents two examples (upper and lower panels) of macrophages observed under confocal and then FE-SEM. For the observation by confocal microscopy, cells were immunostained with combined LAMP1/LAMP2 antibodies (red channels), *L. amazonensis*-specific antibody (2A3-26, green channels) and stained with DAPI (blue channel). Extruded amastigotes are indicated by letters a, b and c. In the lower panel, the confocal images are presented in different focal planes to show the indicated amastigote extrusions. The membrane covering the extruding amastigotes (A) is observed at higher magnification and resolution in these two examples and displays a smooth aspect with no evident pores. The same extrusion observed by confocal microscopy revealed that extruded amastigotes are fully covered with LAMPs. Bars = 2 μm.
Results are representative of four (A–B) and two (C–D) experiments.

We quantified the percentage of MEF-derived amastigotes associated with PV components by flow cytometry, using LIMP1 as PV marker. Around 25% of amastigotes were LIMP1-positive, indicating association with host cell PV membranes; this percentage was found in amastigotes isolated from MEF-WT and MEF-LAMP1/2 KO (Fig. 5C). Flow cytometry quantification of LIMP1-positive amastigotes employed antibody isotype and secondary immunostaining controls for LIMP1 (Supplementary Figs S2E and F and S3D). Thus, we obtained preparations of amastigotes associated with host phagolysosomal components (LIMP1 positive), mimicking parasite-containing host cell extrusions, which display or are devoid of LAMP1/LAMP2 proteins (after amastigote isolation from MEF-WT and MEF-LAMP1/2KO respectively).

 

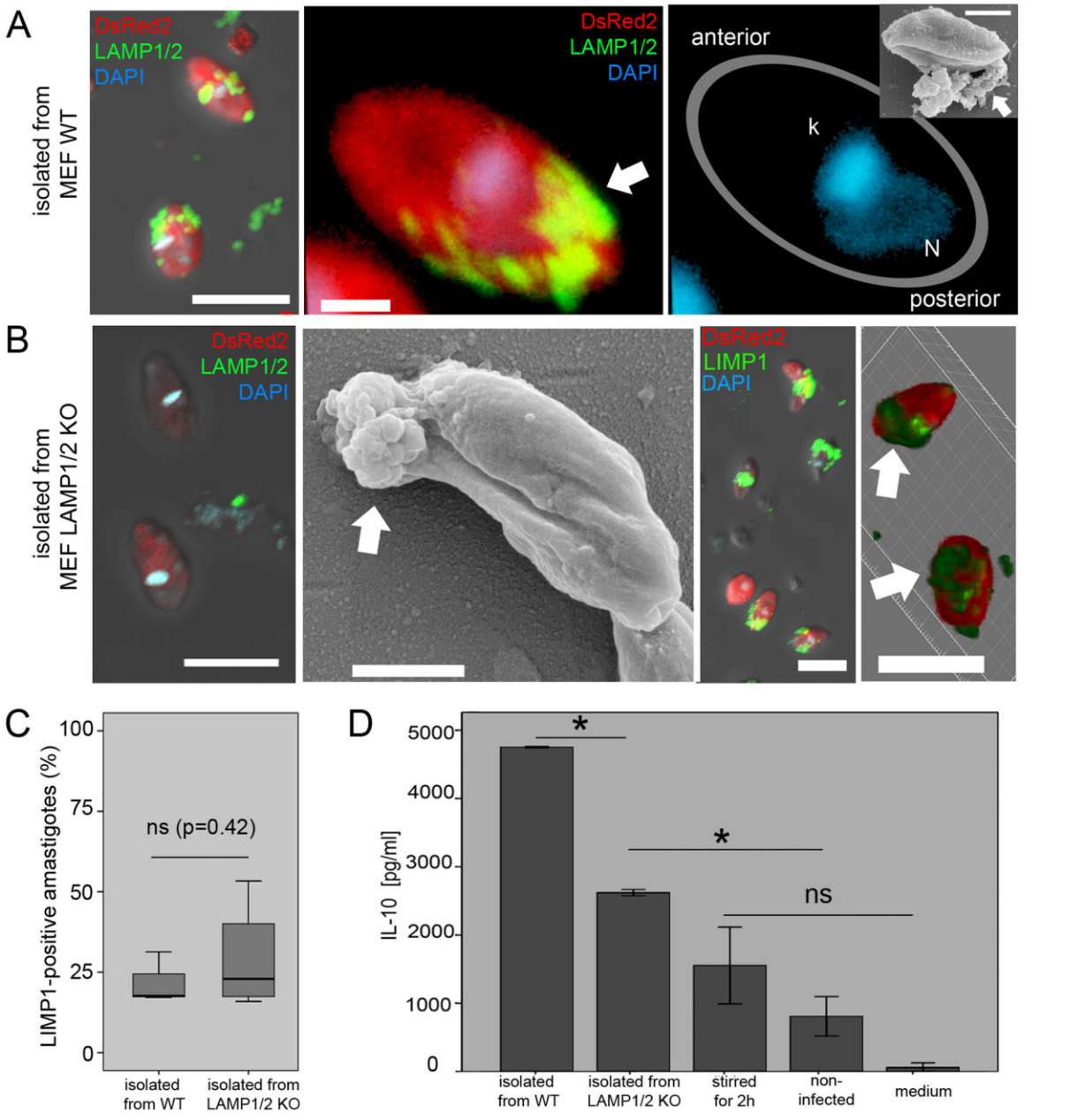


**Fig. 5.** Fibroblast-derived amastigotes associated with LAMP stimulate interleukin-10 (IL-10) production by macrophages.
A. *L. amazonensis*-DsRed2 amastigotes (red) isolated from wild-type mouse embryonic fibroblasts (MEF-WT) preserved LAMP1 and LAMP2 proteins (immunostained with LAMP1/LAMP2 antibodies, green) on their surfaces. First image: DIC merged with green, red and blue (DAPI) channels, bar = 5 μm. Second and third images: three-dimensional reconstructions of an amastigote showing LAMP cap at the parasite posterior pole (arrow). The position of parasite nucleus (N) and kinetoplast (k) indicate amastigote polarity. Bar = 1 μm. Inset: field-emission scanning electron microscopy (FE-SEM) of an amastigote and associated membrane debris (arrow) at the posterior pole, bar = 2 μm.
B. *L. amazonensis*-DsRed2 amastigotes (red) isolated from LAMP1/LAMP2 knockout MEF. First image show DIC merged green, red and blue (DAPI) channels of amastigotes incubated with LAMP1/LAMP2 antibodies (green): amastigotes are devoid of a LAMP cap on their surfaces, bar = 5 μm; second image acquired by FE-SEM reveals membrane debris at their posterior poles, bar = 2 μm. Third and fourth images: immunostaining of LIMP1 (green) revealed that the membrane cap on the amastigote surface conserves lysosomal components; three-dimensional reconstruction of amastigotes (fourth image) shows LIMP cap on parasite poles (arrows), bar = 5 μm.
C. Flow cytometry quantification of the percentage of amastigotes positive for LIMP-1. Amastigotes were isolated from MEF-WT or MEF-LAMP1/2KO, after 48 h of infection. LIMP-1 is presented on approximately 20% of amastigotes ($P > 0.05$, ANOVA).
D. IL-10 production by BMDMØ cultures infected with amastigotes isolated from MEF-WT (LAMP-associated) or from MEF-LAMP1/LAMP2 KO (LAMP-devoid amastigotes); medium alone, non-infected macrophage cultures and amastigotes cultivated under agitation for 2 h (stirred amastigotes) were employed as experimental controls. LAMP-associated amastigotes stimulate a higher production of IL-10 when compared with LAMP-devoid parasites, which, in turn, induce a higher production of the cytokine when compared with control groups. ANOVA, $P < 0.05$. Data representative of three independent experiments.

 

These preparations of LAMP-positive or LAMP-negative amastigotes were added to fresh BMDMØ cultures and IL-10 production was assessed (Fig. 5D and E). When interacting with amastigotes displaying LAMP1/LAMP2-rich host membrane caps, macrophages produce higher amounts of IL-10 when compared with the interaction with amastigotes devoid of LAMP (Fig. 5D). Stirred amastigotes (cultivated under mild agitation), devoid of host membrane caps, induced a lower IL-10 production (comparable to non-infected macrophages). In some experiments LAMP-devoid amastigotes induced an intermediate IL-10 production by macrophages, not so pronounced as that induced by LAMP-positive amastigotes but higher than baseline production of non-infected macrophages. This suggests that additional host cell membrane components attached to amastigotes could stimulate IL-10 production by macrophages.

## Discussion

The spreading of amastigotes to vicinal cells and tissues represent a much-unexplored topic in *Leishmania* biology. Here we demonstrate that *L. amazonensis* amastigotes are extruded from affected macrophages presenting apoptotic-like features and are often rescued by vicinal macrophages *in vitro*. We propose that this intracellular parasite carries host cell components during its extrusion, an event that has important implications for the pathogenesis of *Leishmania* and possibly other intracellular parasites adapted to and interactive with parasitophorous vacuoles. By conserving host cell components on their surfaces, parasites could evade host immune systems, modulating cytokine production.

Cell-to-cell transfer of *Leishmania* could be the preferential way of parasite spreading *in vivo*. The exchange of amastigotes between host cells would occur in a cascade of events, involving diversified cell lineages and culminating in the intracellular growth within macrophages. Peters and colleagues studied the context of transfer of *L. major* promastigote forms from the sand fly *Phlebotomus duboscqi* to mice (Peters *et al*., 2008). They observed by multiphoton intravital microscopy (MP-IVM) the migratory behaviour of host neutrophils at the site of insect bite and concluded that these cells are essential for the establishment of the parasite after host-to-host transfer. Additionally, they present flow cytometry data showing that parasites once hosted by neutrophils after 18 h of post-intradermal inoculation of promastigotes were found in macrophages after 6 days. Ng and colleagues using the same live imaging techniques have shown that dendritic cells responded to *L. major* infection in a similar manner (Ng *et al*., 2008). Thus, it is possible to conceive neutrophils, dendritic cells and other host cells as amastigote deliverers to macrophages, sheltering the parasite in customized PVs until the transmission. For instance, *Leishmania donovani* promastigotes are maintained in non-lytic compartments of neutrophils and are transferred to macrophages when the latter internalize infected and apoptotic neutrophils, a process regarded as a Trojan horse tactic (Gueirard *et al*., 2008). These data suggest that cell-to-cell parasite transfer without exposure to extracellular milieu could represent an important requirement, at least in the first hours of infection, for parasite establishment.

We present evidence that, although unable to halt the expression of the pro-apoptotic Bax gene in long-term cultivated macrophages, *L. amazonensis* amastigotes increased the expression of anti-apoptotic genes such as Bcl-2 and IGF-I. Our results suggest an elegant strategy of *Leishmania* intracellular parasitism: delay or inhibit host cell apoptosis to endure, but ultimately exploit and benefit from host cell apoptosis-like damage to spread. The association between host cell apoptosis and *Leishmania* spreading for other parasite species and cell lineages requires further investigation (Getti *et al*., 2008). The importance of host cell apoptosis for amastigote cell-to-cell spreading was strongly suggested by micro-irradiation of infected macrophages, which selectively induce apoptosis-like cell death of predefined macrophages, allowing and triggering non-irradiated vicinal macrophages to rescue parasites from dying, irradiated cells.

Our results discard a parasite multiplication burst of host cells. We hypothesize that amastigote populations hosted by macrophages for long periods of time would stabilize due to nutrient restriction (after parasite population increase) or by expression of a number of host cell factors. In this line, in experimental visceral leishmaniasis in hamsters, *Leishmania chagasi* amastigote apoptosis was observed in spleen and liver in the late period of infection, suggesting a parasite population control (Lindoso *et al*., 2004). Further, parasites may present different multiplication rates and spread more or less efficiently among cells *in vitro* depending on the host cell lineage (Hsiao *et al*., 2011).

Pores on macrophage membrane could be formed during this stabilization of amastigote population, without necessarily trigger host cell death. Although *Leishmania* parasites are able to form pores on biological membranes (Noronha *et al*., 2000), and pore formation of macrophages takes place in amastigote transfers (inferred by GFP leakage during transfers and increase in transfer occurrence after SLO treatment of host cells) we did not find evidence of host membrane pores localized on parasite-containing extrusions. Macrophage pores on infected cells possibly participate in parasite cell-to-cell transmission by releasing chemotactic signals to other viable macrophages, which rescue extruded amastigotes.

 

Considering that (i) long-term infected macrophages express increased amounts of IGF-I mRNA, and (ii) IGF-I is implicated in *Leishmania* infections (Reis *et al*., 2013) and in the increased mobilization of inflammatory mononuclear cells to infected sites in footpad lesions (Gomes *et al*., 2000), it is reasonable to assume a participation of IGF-I not only as an important anti-apoptotic factor (Kooijman *et al*., 2002), but also as a chemotactic factor promoting the migration of viable cells towards infected, damaged macrophages. Further studies are needed to explore this specific field that may involve a number of host cell factors influencing migration of cells and phagocytic process.

The parasitophorous extrusions conserve PV components such as LAMPs and Rab7, which are internalized by recipient macrophages together with the rescued amastigotes. The presence of LAMP and possibly other PV components on amastigotes have increased the secretion of IL-10 by recipient macrophages. IL-10 cytokine is known to be secreted by monocytes in response to apoptotic cells (Voll *et al*., 1997), and by neutrophils in response to *L. amazonensis* amastigotes (Carlsen *et al*., 2013). The abnormal presence and/or topology of LAMP in the content of phagolysosomes (as observed during *L. amazonensis* transfer events) could act as a danger associated molecular pattern (DAMPs), triggering IL-10 production; it could also activate signalling pathways related to recognition of apoptotic/necrotic bodies, leading to anti-inflammatory immune responses which involves IL-10 and TGF-β.

IL-10 is implicated in susceptibility and chronicity of *Leishmania mexicana in vivo* (Buxbaum and Scott, 2005). Wanderley *et al*. (2006) demonstrated that the induction of IL-10 mRNA expression and increased TGF-β secretion due to *L. amazonensis* infection was correlated with the increase of phosphatidylserine (PS) exposure on amastigote surface, thus establishing that amastigotes mimic an apoptotic cell to subvert host immune functions and prevail. Mass spectrometry evidenced that *Leishmania promastigotes* do not constitutively produce PS but its presence is conceded on other growth phases (Weingärtner *et al*., 2012). However the observation made here that amastigotes remain associated with immunomodulatory host membrane remnants suggests that part of PS displayed by parasites comes from an exogenous origin.

Although we present a solid evidence of an anti-inflammatory stimulus mediated by exposition of LAMP on amastigotes, distinct immunomodulatory features of amastigotes extracted from different host cells must not be discarded.

The parasitophorous extrusions displayed by *L. amazonensis* were similar to other pathogen host cell egress mechanisms. These mechanisms, involving or not involving host cell death, include pathogen exocytosis, extrusion or expulsion from the host. The bacteria *Chlamydia* exit host cells after host cell lysis mediated by proteases or after a non-lytic, actin-dependent extrusion from the host cell. In this process, the bacteria are extruded in a double-membrane vesicle generated from the bacterial intracellular vacuole and cytoplasmic membranes (Hybiske and Stephens, 2007). *Legionella pneumophila* express two proteins (LepA and LepB) homologous to host SNARE proteins. This homology allows the subversion of native host cell intracellular trafficking and vesicle fusion by these bacterial products, favouring the non-lytic exocytosis of *L. pneumophila* from host cells (Chen *et al*., 2004; 2007). During *in vitro* cell-to-cell transmission, *Mycobacterium marinum* and *M. tuberculosis* are ejected from host cells through an F-actin-rich structure denominated ejectosome (Hagedorn *et al*., 2009); the bacteria also remain associated with membrane remnants in the process. Viruses such as human immunodeficiency virus (HIV) have also developed non-lytic strategies to egress from host cells. In macrophages, HIV egress can be mediated by Trojan exosomes, originating in multivesicular bodies (MVB) that retain common endosomal and MVB proteins (Gould *et al*., 2003; Chertova *et al*., 2006). The fungus *Cryptococcus neoformans* escape from host cells by an active, pathogen-driven extrusion/expulsion process, apparently without damaging the host (Alvarez and Casadevall, 2006). The fungus can be transferred from cell to cell without exposure to the extracellular milieu; however, the process is still poorly understood and the underlying mechanisms unknown (Alvarez and Casadevall, 2007).

This experimental work proposes a novel mechanism of host cell exit for *Leishmania* amastigotes, an issue extensively neglected in the study of these parasites. It is now possible to investigate this dynamic phenomenon due to live imaging advances, some of them employed very advantageously in this study, during *in vitro* experiments. To extend these observations in *ex vivo* live imaging of infected tissue slices and intra-vital imaging are future challenges and will certainly reveal additional aspects of amastigote egress and reinfection.

## Experimental procedures

### *Parasites and host cells*

*Leishmania* amastigotes were isolated from BALB/c mice footpad lesions after 2 months of amastigote subcutaneous inoculation (Rabinovitch *et al*., 1986). The parasites employed in this study were wild type (WT) or *Discosoma* sp. red fluorescent protein-2 (DsRed2)-transfected *L.* (*L.*) *amazonensis* LV79 strain (MPRO/BR/72/M1841) and green fluorescent protein (GFP)-transfected *L.* (*L.*) *amazonensis* M2269 strain (MHOM/BR/1973/M2269).

BALB/c, C57BL/6 and C57BL/6-GFP mice (8 weeks of age) were used as the source of bone marrow macrophage precursors, which differentiate into macrophages on plastic Petri dishes in the presence of RPMI 1640 medium supplemented with 20% fetal bovine serum, 100 U $m^{-1}$ penicillin, 100 μg $ml^{-1}$ streptomycin and 30% of L929 cell conditioned medium for 6 days at 37°C, 5% $CO_2$ (De Souza Leao *et al*., 1995). Differentiated bone marrow-derived macrophages (BMDMØ) were detached from Petri dishes by incubation with 0.01 M phosphate-buffered saline (PBS) pH 7.2 supplemented with 20 mM Hepes and 1% EDTA for 20 min. BMDMØ were collected by flushing dishes with warmed Hanks' Buffered Salt Solution (HBSS, Sigma-Aldrich). Cells were counted and distributed in 24-well plates, Mattek (Mattek Corporation) or ibidi Hi-Q4 (ibidi GmbH) round dishes, both pre-treated for cell culture, where they were cultivated in RPMI 1640 medium supplemented with 10% fetal bovine serum, 100 U $m^{-1}$ penicillin, 100 μg $ml^{-1}$ streptomycin (complete medium) and 5% of L929 cell conditioned medium.

RAW 264.7 macrophage-like lineage cells (ATCC) were cultivated in complete medium; the liposomal transfection of RAW 264.7 macrophage-like cells was performed using FuGene HD transfection reagent (Roche Applied Science) and the following plasmids: LAMP1-GFP (kindly donated by Dr Norma Andrews, Maryland University, USA), Rab7-GFP and LifeAct-RFP F-actin marker (ibidi GmbH). Macrophages were cultivated on Mattek or ibidi Hi-Q4 round dishes suitable for live cell imaging and placed in incubators fitted on microscope stages.

Immortalized C57BL/6 mouse embryonic fibroblasts (MEF) were kindly donated by Dr Paul Saftig (Biochemisches Institute, Christian-Albrechts-Universität zu Kiel, Germany). In this study we employed the PS1 wild-type fibroblasts (MEF-WT) and the #79 LAMP1/LAMP2 double knockout fibroblasts (MEF-LAMP1/LAMP2 KO), which were immortalized by the same protocol (Eskelinen *et al*., 2004). These cells were maintained in 75 $cm^2$ culture bottles, pre-treated for cell culture.

### *Infection of host cells*

*Leishmania amazonensis* amastigotes were added to macrophage cultures in multiplicity of infection (moi) of 5:1 and incubated at 34°C, 5% $CO_2$ in complete medium for 2 h for host cell-parasite interaction. Amastigotes at moi 20:1 were added to RAW 264.7 cultures after 24 h of transfection and incubated at 34°C, 5% $CO_2$ in complete medium for 6 h for interaction. Amastigotes at moi 20:1 were added to MEF cultures in culture flasks and incubated at 34°C, 5% $CO_2$ in complete medium for 24 h for interaction.

After this interaction period, free parasites were removed from cell cultures by washing with HBSS; then cultures were incubated in complete medium at 34°C, 5% $CO_2$ atmosphere for additional 24 h (MEF and RAW 264.7 cultures) or for up to 30 days (BMDMØ cultures).

For long-term experiments (> 4 days), BMDMØ cultures were maintained at 34°C, 5% $CO_2$ and medium was replaced every 4 days and also before each microscopic recording. Viability of *L. amazonensis* amastigotes hosted by BMDMØ during long-term cultivation was inferred by the maintenance of enlarged parasite-containing PVs and amastigote fluorescence (in the case of parasites expressing fluorescent proteins).

### *Infection of BMDMØ with amastigotes associated with or devoid of host cell LAMP*

MEF cells were used as transient hosts for *Leishmania* amastigotes for 48 h, cultivated in DMEM medium supplemented with 10% fetal bovine serum, 100 U $m^{-1}$ penicillin, 100 μg $ml^{-1}$ streptomycin at 34°C, 5% $CO_2$. After this incubation period, infected MEF cells were scrapped from culture bottles and mechanically disrupted through a 15 ml potter homogenizer. Then the suspension containing disrupted cells was passed 10 times through 30G needles. Amastigotes were collected from suspensions of disrupted MEF-WT or MEF-LAMP1/LAMP2 KO cells by employing the standard amastigote isolation protocol (Rabinovitch *et al*., 1986), without overnight or stirred incubation to preserve host cell membranes associated with amastigotes (Saraiva *et al*., 1983). The amastigotes isolated from MEF cells were added to C57BL/6 BMDMØ cultures in 24-well plates at 20:1 multiplicity, which were then incubated for 72 h at 34°C, 5% $CO_2$ in complete medium containing 5% L929 conditioned medium and 100 ng $ml^{-1}$ of lipopolysaccharide (LPS, Sigma-Aldrich). After this period, BMDMØ supernatants were collected and stored at −80°C until cytokine production evaluation.

### *Multidimensional live cell imaging*

Multidimensional imaging of infected macrophage cultures was performed using a Leica SP5 II Tandem Scanner system (Leica Microsystems). Images were acquired from cells cultivated and infected in Mattek or ibidi dishes, placed in the incubator coupled to the microscope. The incubator maintains temperature and $CO_2$ condition throughout the image acquisition.

Fluorescence and differential interference contrast (DIC) images were acquired at resonant scanning mode, 512 × 512 or 1024 × 1024 resolution, using 63× (HCX PL APO 63×/1.40–0.60 CS λ-BL) or 100× (HCX PL APO 100×/1.44 CORR CS) oil immersion objectives and z-stacks ranging from 0.3 to 0.5 μm. To avoid phototoxicity, lasers were set to no more than 5% of potency; additionally, the duration of z-stack acquisition, for each position and in each time point, was 30 s at maximum (to avoid prolonged exposure).

After acquisition, images were processed by Imaris v.7.4.2 software (Bitplane AG, Andor Technology), which allowed for the construction of multidimensional images integrating spatial (tridimensional) and temporal data (acquisition of the same microscopic field in defined time intervals). Images were visualized applying Blend, maximum intensity projection (MIP) or hue-saturation-value filters.

In some experiments, macrophages were stained with Hoechst 3 3342 (Invitrogen, Life Technologies) in order to identify host cell nuclei. Macrophage nuclei fluorescence signals allowed for automatic quantification of host cells in multidimensional images by the Imaris program. Based on Hoechst staining, the software creates isosurfaces representative of macrophage nuclei (Real and Mortara, 2012) and automatically counts these isosurfaces per time point in different microscopic fields. Software attributes a yellow square to each counted nuclei. Parameters for Hoechst-based isosurfaces construction include background subtraction, track surfaces and no split objects. Transfer of amastigotes between macrophages was counted by direct observation of multidimensional images. A transfer event is counted when one macrophage transfers amastigotes to another one, independent

 

of how many amastigotes were transferred. Tracking of transferred amastigotes were performed in some cases, to improve the visualization of the events: in this approach, the DsRed signal of *L. amazonensis* amastigotes hosted by donor macrophages was tracked using Imaris isosurface tracking tools. The software attribute isospots for each amastigotes and a line tracing of isospots displacement in multidimensional images.

Multichamber dishes (Hi-Q4 dishes, ibidi GmbH, pre-treated for cell culture) were used for experiments in which more than one experimental condition was observed in the same microscope acquisition session. Multichamber dishes were used in experiments with infected and non-infected macrophages and in experiments with infected macrophage cultures (20 days of infection) treated or not treated with 50 ng $ml^{-1}$ Streptolysin O (SLO), which was washed from cultures after a pulse of 20 min in calcium-free PBS. Production and purification of SLO were performed as established, using plasmids kindly donated by Dr Rodney Tweten (University of Oklahoma, USA) and kindly made available to us by Dr Norma W. Andrews (University of Maryland, USA) (Idone *et al.*, 2008).

### *Immunostaining and ELISA assays*

Previous to cell cultivation, glass coverslips were washed with neutral detergent, water and ethanol, and autoclave sterilized. Coverslips containing infected macrophages or amastigote suspensions in 1.5 ml microcentrifuge tubes (derived from MEF host cells or mouse footpad lesions) were washed and fixed for 1 h with 3.5% paraformaldehyde in PBS at room temperature. LAMP1 and LAMP2 proteins were immunostained using monoclonal antibodies obtained from DSHB (1D4B and ABL-93 hybridomas, Iowa University, USA). LIMP1 immunostaining of these structures was performed using anti-CD63 (LIMP1) monoclonal antibodies (US Biological, Massachusetts, USA). LAMP and LIMP antibody specificities were confirmed by employing isotype control antibodies (rat IgG1 and IgG2A primary antibodies) or only secondary antibodies. Amastigotes were immunostained with 2A3-26 antibody conjugated to FITC (kindly donated by Dr Eric Prina, Institut Pasteur, France). Primary and secondary antibodies (Alexa Fluor™) were incubated for 1 h before an additional stain with 10 μM 4′,6-diamidino-2-phenylindole (DAPI, Invitrogen, Life Technologies) for 15 min. Confocal images of the samples were acquired with a 63× or 100× oil immersion objective in the Leica SP5 II TS system and processed by the Imaris program using Blend filters. Flow cytometry analysis of immunostained amastigotes were performed on BD FACSCanto or BD Accuri C6 instruments (BD Biosciences).

Mouse interleukin 10 Enzyme-Linked Immunosorbent Assay kit (ELISA Ready-SET-Go!, eBioscience) was used for the measurement of cytokine production of BMDMØ culture supernatants, according to manufacturer's instructions.

### *Micro-irradiation of infected cells*

Macrophages obtained from C57BL/6-GFP mice or transfected RAW 264.7 macrophages were infected with *L. amazonensis*-DsRed2 amastigotes for 24 to 96 h and cultivated in round dishes, suitable for the incubator coupled to the Leica SP5 II TS system. Using the Leica FRAP Wizard tool provided by the acquisition software, we delimited an area or a region of interest (ROI), in which laser pulses were applied. These ROI corresponded to Hoechst-stained macrophage nuclear regions, adjusting the focal plane (z axis) to the centre of the nuclei; a concentrated near-ultraviolet (UV) laser [405 nm, at 100% power (50 mW) and 400 Hz frequency] was applied to the ROI for 300–500 s before multidimensional live recordings (Soustelle *et al.*, 2008). The technique was also employed to hasten the extrusion of amastigotes from RAW transfected cells, which are not suitable for long-term *in vitro* infection (i.e. for more than 5 days).

To check whether micro-irradiation is inducing apoptosis, micro-irradiation of 48 h infected BMDMØ cultures was performed in complete medium supplemented with 5% of L929 cell conditioned medium, 2.5 mM $CaCl_2$, 500 nM of nuclear probe YO-PRO-1 Iodide (Molecular Probes) and 2.5 μg $ml^{-1}$ of Annexin V-CF633 (Biotium).

### *Electron microscopy and correlative imaging*

Suspensions of macrophages infected for 20 days with *L. amazonensis* were fixed in a solution of 2.5% glutaraldehyde and 2% formaldehyde in 0.1 M sodium cacodylate buffer at room temperature for 1 h, then stored at 4°C before conventional transmission electron microscopy (TEM) procedures (Arruda *et al.*, 2012). Samples were observed in a Jeol 100 CX II electron microscope. For SEM, infected macrophages or isolated amastigotes were incubated in Mattek dishes and fixed with 3.5% paraformaldehyde according to established preparation protocols. Briefly, fixed samples were washed in 0.1 M cacodylate solution, post-fixed with osmium tetroxide, treated with tannic acid, dehydrated with ethanol and then dried in a CPD 030 critical point dryer. The dishes were coated with a gold layer using a sputtering method. Samples were observed in a Field Emission FEI Quanta FEG 250 scanning electron microscope.

In order to observe and acquire images from the same infected macrophage in confocal and SEM instruments, cells were cultivated on gridded dishes (ibidi u-Dish 35 mm Grid-500 ibiTreat; ibidi GmbH) suitable for observation in the Leica SP5 II TS confocal as well as the Field Emission SEM. The grid presents alpha-numerical co-ordinates and gridded markings spaced by 500 μm. Samples were immunostained and observed by confocal microscopy prior to preparation for observation by electron microscopy.

### *Quantitative PCR for the expression of pro- and anti-apoptotic macrophage genes*

To evaluate the expressions of pro- and anti-apoptotic macrophage genes, total RNA was extracted from $2 \times 10^5$ cells $ml^{-1}$ using TRIzol (Invitrogen, USA), following the manufacturer's protocol (RNA integrity was determined as an OD260/280 absorption ratio between 1.8 and 2.1). Then 1 μg of purified RNA was mixed with 10 μl of a solution consisting of a basic buffer (100 mM Tris-HCl, pH 8.3, containing 500 mM KCl and 15 mM $MgCl_2$ Invitrogen, USA), dNTP (10mM; Fermentas, USA), random primers (Invitrogen, USA), OligoDT primers (Invitrogen, USA), RNaseOUT recombinant ribonuclease inhibitor (40 U $\mu l^{-1}$; Invitrogen, USA), M-MLV reverse transcriptase (100 U $\mu l^{-1}$). The reactions were incubated at 37°C for 50 min and were denatured at 70°C for 15 min.

For real-time quantitative RT-PCR, the following primers set were designed: murine Bax gene (GenBank Accession No. NM007527), forward: 5′-GGC CTT TTT GCT ACA GGG TTT CAT-3′ and reward: 5′-TGC TGT CCA GTT CAT CTC CAA TTC-3′; for murine Bcl-2 gene, forward: 5′-GAC TGA GTA CCT GAA CCG GCA TCT-3′ and reward: 3′-AAG CCC AGA CTC ATT CAA CCA GAC-3′ (GenBank Accession No. NM009741), and for murine IGF-I, forward, 5′-TAC TTC AAC AAG CCC ACA GG-3′ and reward, 5′-AGT CTT GGG CAT GTC AGT GT-3′ (GenBank Accession No. NM010512). β-Actin (GenBank Accession No. NM00739) was used as a constitutively expressed control gene for normalization (primers: forward, 5′-GCC TTC CTT CTT GGG TAT GGA ATC-3′ and reward, 5′-ACG GAT GTC AAC GTC ACA CTT CAT-3′). The reactions included master mix Syber Green (2×) (Applied Biosystems, USA) and 1 μl cDNA (1 μg) template and were run in triplicate on a real-time PCR system (StepOne; Applied Biosystems, USA). The PCR conditions were the same for all primer combinations: 95°C for 10 min, 40 cycles of 92°C for 2 min, 57.5°C for 30 s and 70°C for 30 s. After PCR amplification, a melting curve was generated to confirm the specificity of the products. The data were presented as a relative quantification and were calculated using $2^{-\Delta\Delta Ct}$ (Pfaffl, 2001).

### *Statistics*

All statistical tests employed in this study were performed by SPSS software (SPSS). These tests included the Student's *t*-test and analysis of variance (ANOVA) with Bonferroni *post-hoc* tests. Results represent data obtained in at least two experiments and at least in duplicate.

## Acknowledgements

This study was supported by funds from Fundação de Amparo à Pesquisa do Estado de São Paulo (FAPESP post-doctoral fellowship 10/19335-4). FR acknowledges the ever-present advice and mentoring of Professor Michel Rabinovitch and Professor Marcello Barcinski. We would like to thank Cosmas and Damian, Dr Paul Saftig, Dr Eric Prina, Dr Norma Andrews, Dr Lucile Floeter-Winter, Dr Clara Barbiéri, Simone Katz, Dr Denise Arruda, Dr Marcel Lyra, André Aguillera, Carina Carraro and Mônica Gambero for cells and reagent donation, technical support and advice. This manuscript has been proofread and edited by native English speakers with related backgrounds from BioMed Proofreading, LLC.

## References

Alvarez, M., and Casadevall, A. (2006) Phagosome extrusion and host-cell survival after *Cryptococcus neoformans* phagocytosis by macrophages. *Curr Biol* **16:** 2161–2165.

Alvarez, M., and Casadevall, A. (2007) Cell-to-cell spread and massive vacuole formation after *Cryptococcus neoformans* infection of murine macrophages. *BMC Immunol* **8:** 16.

Arruda, D.C., Santos, L.C., Melo, F.M., Pereira, F.V., Figueiredo, C.R., Matsuo, A.L., *et al*. (2012) beta-Actin-binding complementarity-determining region 2 of variable heavy chain from monoclonal antibody C7 induces apoptosis in several human tumor cells and is protective against metastatic melanoma. *J Biol Chem* **287:** 14912–14922.

Buxbaum, L.U., and Scott, P. (2005) Interleukin 10- and Fcgamma receptor-deficient mice resolve *Leishmania mexicana* lesions. *Infect Immun* **73:** 2101–2108.

Carlsen, E.D., Hay, C., Henard, C.A., Popov, V., Garg, N.J., and Soong, L. (2013) *Leishmania amazonensis* amastigotes trigger neutrophil activation but resist neutrophil microbicidal mechanisms. *Infect Immun* **81:** 3966–3974.

Chen, J., de Felipe, K.S., Clarke, M., Lu, H., Anderson, O.R., Segal, G., and Shuman, H.A. (2004) Legionella effectors that promote nonlytic release from protozoa. *Science* **303:** 1358–1361.

Chen, J., Reyes, M., Clarke, M., and Shuman, H.A. (2007) Host cell-dependent secretion and translocation of the LepA and LepB effectors of *Legionella pneumophila*. *Cell Microbiol* **9:** 1660–1671.

Chertova, E., Chertov, O., Coren, L.V., Roser, J.D., Trubey, C.M., Bess, J.W., Jr, *et al*. (2006) Proteomic and biochemical analysis of purified human immunodeficiency virus type 1 produced from infected monocyte-derived macrophages. *J Virol* **80:** 9039–9052.

Christophers, S.R. (1904) On a parasite found in persons suffering from enlargement of spleen in India, Second Report. In *Scientific Memoirs by Officers of the Medical and Sanitary Departments of the Government of India*.

Courret, N., Frehel, C., Gouhier, N., Pouchelet, M., Prina, E., Roux, P., and Antoine, J.C. (2002) Biogenesis of *Leishmania*-harbouring parasitophorous vacuoles following phagocytosis of the metacyclic promastigote or amastigote stages of the parasites. *J Cell Sci* **115:** 2303–2316.

De Souza Leao, S., Lang, T., Prina, E., Hellio, R., and Antoine, J.C. (1995) Intracellular *Leishmania amazonensis* amastigotes internalize and degrade MHC class II molecules of their host cells. *J Cell Sci* **108:** 3219–3231.

Dedet, J.P. (2007) [Edmond Sergent's discoveries on the vectorial transmission of agents of human and animal infectious diseases]. *Bull Soc Pathol Exot* **100:** 147–150.

Eischen, A., Vincent, F., Bergerat, J.P., Louis, B., Faradji, A., Bohbot, A., and Oberling, F. (1991) Long term cultures of human monocytes *in vitro*. Impact of GM-CSF on survival and differentiation. *J Immunol Methods* **143:** 209–221.

Eskelinen, E.L., Schmidt, C.K., Neu, S., Willenborg, M., Fuertes, G., Salvador, N., *et al*. (2004) Disturbed cholesterol traffic but normal proteolytic function in LAMP-1/LAMP-2 double-deficient fibroblasts. *Mol Biol Cell* **15:** 3132–3145.

Fernandes, M.C., Cortez, M., Flannery, A.R., Tam, C., Mortara, R.A., and Andrews, N.W. (2011) *Trypanosoma cruzi* subverts the sphingomyelinase-mediated plasma membrane repair pathway for cell invasion. *J Exp Med* **208:** 909–921.

Florentino, P.T.V., Real, F., Bonfim-Melo, A., Orikaza, C.M., Ferreira, E.R., Pessoa, C.C. *et al*., (2014) An historical perspective on how advances in microscopic imaging contributed to understanding the *Leishmania* Spp. and Trypanosoma cruzi host-parasite relationship. *BioMed Research International*. DOI: 10.1155/2014/565291

Getti, G.T., Cheke, R.A., and Humber, D.P. (2008) Induction of apoptosis in host cells: a survival mechanism for *Leishmania* parasites? *Parasitology* **135:** 1391–1399.

Gomes, C.M., Goto, H., Ribeiro Da Matta, V.L., Laurenti, M.D., Gidlund, M., and Corbett, C.E. (2000) Insulin-like growth factor (IGF)-I affects parasite growth and host cell migration in experimental cutaneous leishmaniasis. *Int J Exp Pathol* **81:** 249–255.

Gould, S.J., Booth, A.M., and Hildreth, J.E. (2003) The Trojan exosome hypothesis. *Proc Natl Acad Sci USA* **100:** 10592–10597.

Gueirard, P., Laplante, A., Rondeau, C., Milon, G., and Desjardins, M. (2008) Trafficking of *Leishmania donovani* promastigotes in non-lytic compartments in neutrophils enables the subsequent transfer of parasites to macrophages. *Cell Microbiol* **10:** 100–111.

Hagedorn, M., Rohde, K.H., Russell, D.G., and Soldati, T. (2009) Infection by tubercular mycobacteria is spread by nonlytic ejection from their amoeba hosts. *Science* **323:** 1729–1733.

Heyneman, D. (1971) Immunology of leishmaniasis. *Bull World Health Organ* **44:** 499–514.

Hsiao, C.H., Ueno, N., Shao, J.Q., Schroeder, K.R., Moore, K.C., Donelson, J.E., and Wilson, M.E. (2011) The effects of macrophage source on the mechanism of phagocytosis and intracellular survival of *Leishmania*. *Microbes Infect* **13:** 1033–1044.

Hybiske, K., and Stephens, R.S. (2007) Mechanisms of host cell exit by the intracellular bacterium *Chlamydia*. *Proc Natl Acad Sci USA* **104:** 11430–11435.

Idone, V., Tam, C., Goss, J.W., Toomre, D., Pypaert, M., and Andrews, N.W. (2008) Repair of injured plasma membrane by rapid $Ca^{2+}$-dependent endocytosis. *J Cell Biol* **180:** 905–914.

Kooijman, R., Coppens, A., and Hooghe-Peters, E. (2002) Igf-I inhibits spontaneous apoptosis in human granulocytes. *Endocrinology* **143:** 1206–1212.

Lindoso, J.A., Cotrim, P.C., and Goto, H. (2004) Apoptosis of *Leishmania* (*Leishmania*) *chagasi* amastigotes in hamsters infected with visceral leishmaniasis. *Int J Parasitol* **34:** 1–4.

Meleney, H.E. (1925) The histopathology of kala-azar in the hamster, monkey, and man. *Am J Pathol* **1:** 147–168 111.

Ng, L.G., Hsu, A., Mandell, M.A., Roediger, B., Hoeller, C., Mrass, P., *et al*. (2008) Migratory dermal dendritic cells act as rapid sensors of protozoan parasites. *PLoS Pathog* **4:** e1000222.

Noronha, F.S., Cruz, J.S., Beirão, P.S., and Horta, M.F. (2000) Macrophage damage by *Leishmania amazonensis* cytolysin: evidence of pore formation on cell membrane. *Infect Immun* **68:** 4578–4584.

Peters, N.C., Egen, J.G., Secundino, N., Debrabant, A., Kimblin, N., Kamhawi, S., *et al*. (2008) *In vivo* imaging reveals an essential role for neutrophils in leishmaniasis transmitted by sand flies. *Science* **321:** 970–974.

Pfaffl, M.W. (2001) A new mathematical model for relative quantification in Real-Time RT-PCR. *Nucleic Acids Res* **29:** 2002–2007.

Rabinovitch, M., and De Stefano, M.J. (1973) Particle recognition by cultivated macrophages. *J Immunol* **110:** 695–701.

Rabinovitch, M., Zilberfarb, V., and Ramazeilles, C. (1986) Destruction of *Leishmania mexicana* amazonensis amastigotes within macrophages by lysosomotropic amino acid esters. *J Exp Med* **163:** 520–535.

Real, F., and Mortara, R.A. (2012) The diverse and dynamic nature of *Leishmania* parasitophorous vacuoles studied by multidimensional imaging. *PLoS Negl Trop Dis* **6:** e1518.

Reis, L.C., Ramos-Sanchez, E.M., and Goto, H. (2013) The interactions and essential effects of intrinsic insulin-like growth factor-I on *Leishmania* (*Leishmania*) *major* growth within macrophages. *Parasite Immunol* **35:** 239–244.

Ridley, D.S. (1980) A histological classification of cutaneous leishmaniasis and its geographical expression. *Trans R Soc Trop Med Hyg* **74:** 515–521.

Rittig, M.G., and Bogdan, C. (2000) *Leishmania*–host-cell interaction: complexities and alternative views. *Parasitol Today* **16:** 292–297.

Rittig, M.G., Schroppel, K., Seack, K.H., Sander, U., N'Diaye, E.N., Maridonneau-Parini, I., *et al*. (1998) Coiling phagocytosis of trypanosomatids and fungal cells. *Infect Immun* **66:** 4331–4339.

Saraiva, E.M., Pimenta, P.F., Pereira, M.E., and de Souza, W. (1983) Isolation and purification of amastigotes of *Leishmania mexicana* amazonensis by a gradient of Metrizamide. *J Parasitol* **69:** 627–629.

Soustelle, L., Aigouy, B., Asensio, M.L., and Giangrande, A. (2008) UV laser mediated cell selective destruction by confocal microscopy. *Neural Develop* **3:** 11.

Theodorides, J. (1997) [Historical note on the discovery of cutaneous leishmaniasis transmission by Phlebotomus]. *Bull Soc Pathol Exot* **90:** 177–178.

Tweten, R.K. (2005) Cholesterol-dependent cytolysins, a family of versatile pore-forming toxins. *Infect Immun* **73:** 6199–6209.

Voll, R.E., Herrmann, M., Roth, E.A., Stach, C., Kalden, J.R., and Girkontaite, I. (1997) Immunosuppressive effects of apoptotic cells. *Nature* **390:** 350–351.

Wanderley, J.L., Moreira, M.E., Benjamin, A., Bonomo, A.C., and Barcinski, M.A. (2006) Mimicry of apoptotic cells by exposing phosphatidylserine participates in the establishment of amastigotes of *Leishmania* (*L*) *amazonensis* in mammalian hosts. *J Immunol* **176:** 1834–1839.

Weingärtner, A., Kemmer, G., Müller, F.D., Zampieri, R.A., Gonzaga dos Santos, M., Schiller, J., and Pomorski, T.G. (2012) *Leishmania* promastigotes lack phosphatidylserine but bind annexin V upon permeabilization or miltefosine treatment. *PLoS ONE* **7:** e42070.

WHO (2010) Control of the leishmaniasis. In *WHO Technical Report Series*. Geneva: WHO Press.

Winter, G., Fuchs, M., McConville, M.J., Stierhof, Y.D., and Overath, P. (1994) Surface antigens of *Leishmania mexicana* amastigotes: characterization of glycoinositol phospholipids and a macrophage-derived glycosphingolipid. *J Cell Sci* **107** (Part 9)**:** 2471–2482.

Wright, J.H. (1903) Protozoa in a case of tropical ulcer ('Delhi Sore'). *The J Med Res* **10:** 472–482 477.

## Supplemental information

Additional Supporting Information may be found in the online version of this article at the publisher's web-site:

**Fig. S1.** Host cell pores increased amastigote transfer.
A. BMDMØ-GFP infected with *Leishmania amazonensis*-DsRed2 for 20 days treated with 50 ng $ml^{-1}$ Streptolysin O (SLO), washed

from cultures after a pulse of 20 min in phosphate-buffered saline (PBS) and observed by field-emission scanning electron microscopy (FE-SEM). An amastigote (coloured in red) is exposed by an 8 μm diameter pore on a macrophage surface. Clusters of vesiculated membrane around the pore are suggestive of membrane repair (arrowheads). Bar = 5 μm.

B. Quantification of amastigote transfer events by observation of 10 microscopic fields (63× objective, 150 × 150 μm) under different experimental conditions. Each red dot represents a transfer event detected by multidimensional imaging; we observed more amastigote transfers after SLO treatment during image acquisition period.

C. BMDMØ-GFP infected with *L. amazonensis*-DsRed2 for 20 days treated with 30 μM nocodazole, maintained in medium, and observed by multidimensional imaging. Image acquisition started after 20 days of infection. Treatment with nocodazole induced the formation of blebs containing parasites but not host cell death or cell-to-cell transfer of amastigotes. Images are representative of an infected cell (indicated by white contour) in the presence of the drug; green, red and DIC channels. Bar = 10 μm. Time of image acquisition is represented by days:hours:minutes:seconds: milliseconds (d:hh:mm:ss:sss).

**Fig. S2.** A–B. Correlative imaging of necrotic macrophages extruding amastigotes. Samples were immunostained with a mixture of LAMP1/LAMP2 (lysosome-associated membrane protein) antibodies (red channel), *Leishmania amazonensis*-specific antibody (2A3-26, green channel) and stained with DAPI (blue channel) for observation at the confocal microscope prior to preparation and observation under field-emission scanning electron microscopy (FE-SEM). Extruded amastigotes are indicated by letters a and b observed through these two microscopes.

A. Lower magnification showing two amastigotes (a and b) extruded from necrotic macrophage; the scanning electron micrograph is shown in the left image and two focal planes of the same macrophage are shown in the right.

B. Higher magnification of the extruded amastigotes: while amastigote (b) preserves LAMP on its surface (arrowheads), amastigote (a) is not associated with this lysosomal component. FE-SEM on the left (bars = 10 μm), confocal images (different z-stacks and 3D reconstruction) on the right (bars = 5 μm).

C–D. Isotype control for LAMP1 immunofluorescence, using BMDMØ infected with *L. amazonensis*-DsRed2 for 20 days. In C, LAMP1 antibodies (1D4B hybridomas, a rat IgG2A antibody) were used for immunostaining lysosomal components, followed by a secondary anti-rat antibody conjugated to Alexa Fluor™ 568. In D, a rat IgG2A isotype control was used instead of LAMP1 antibodies, followed by incubation with anti-rat Alexa Fluor™ 568. LAMP1 (red), 2A3-26 (green) and DAPI (blue) fluorescent channels merged with DIC. Bars = 10 μm.

E–F. Isotype control for flow cytometry after LIMP1 immunostaining. Amastigotes isolated from 48 h infected MEF cultures were fixed and incubated with primary antibodies rat IgG1 isotype control (E) and anti-CD63 (LIMP1) antibodies (rat IgG1), followed by incubation with anti-rat secondary antibodies conjugated to Alexa Fluor™ 488.

**Fig. S3.** A. Flow cytometry analysis of lysosomal components on amastigotes isolated from 2-month-old BALB/c footpad lesions; amastigotes were double-stained with mouse LAMP1/LAMP2 and *Leishmania amazonensis*-specific (2A3-26) antibodies. The first scatter plot shows the gating employed in *L. amazonensis* amastigotes population, based on forward (FSC-A) and side scatter (SSC-A) information. The second scatter plot shows the setting of non-fluorescent (negative for LAMP or 2A3-26 antibodies) populations, using non-stained amastigotes. The third scatter plot shows the fluorescence intensities presented by amastigotes immunostained with LAMP and 2A3-26 antibodies. The double-positive population, representing *L. amazonensis* amastigotes that display LAMP caps on their surface, comprises 13.1% of the analysed population of amastigotes. Forth plot shows LAMP and 2A3-26 double-staining of amastigotes cultivated for 2 h on mild agitation (stirred). The percentage of LAMP-positive amastigotes decreased to 4.11%.

B. Transient *L. amazonensis*-DsRed2 infection in wild type (WT) or LAMP1/LAMP2 (lysosome-associated membrane protein) double-knockout mouse embryonic fibroblasts (MEF). Bar = 50 μm.

C. Western blotting for LAMP2 (ABL93 hybridoma) using extracts of MEF-WT and MEF-LAMP1/LAMP2KO. Same results were obtained using anti-LAMP1 antibodies (not shown).

**Video S1.** A. Bone marrow-derived macrophage infected with *Leishmania amazonensis*-DsRed2 for 20 days co-cultured with uninfected RAW macrophage-like cells. RAW cell interacts with hugely infected macrophage and rescue several amastigotes (arrowhead) after the collapse of the latter. Another RAW cell took two amastigotes from the same collapsed macrophage at 1d05:45 time point. Time of image acquisition is represented by days:hours:minutes:seconds:milliseconds (d:hh:mm:ss:sss). Bar = 10 μm.

B. Multidimensional imaging (tridimensional reconstruction plus time) of BMDMØ-GFP infected for 20 days with *L. amazonensis*-DsRed2. Amastigotes (red) are extruded from dying BMDMØ-GFP (green) within zeiotic structures (blebs, arrowheads). At time point 09:53:42, when extrusion formation is more evident, image z-stacks were shown in the video to expose amastigote localization within zeiotic structures. Time of image acquisition is represented by hours:minutes:seconds:milliseconds (hh:mm:ss:sss). Bar = 10 μm. QuickTime .mov file (H.264 codec)

**Video S2.** Quantification of host cells and amastigote transfers in BMDMØ cultures.

A. BMDMØ infected for 15 days with *Leishmania amazonensis*-DsRed2 observed by multidimensional imaging for additional 72 h. The video shows three examples of acquired microscopic fields of an infected culture (out of nine fields in this experiment); DIC of infected macrophages was merged with red and blue fluorescence channels corresponding to *L. amazonensis*-DsRed2 and Hoechst 33342 nuclei staining respectively. The zoom highlights the criterion applied for amastigote transfers quantification. No matter how many amastigotes were rescued by vicinal macrophages, the exchange of parasites between one pair of host cells was quantified as one transfer event. Arrowheads indicate amastigote transfers. In the second example, the region in which a transfer occurs is indicated by white circle.

B. Automated recognition of macrophage nuclei by software analysis, employed to quantify the number of host cell during multidimensional imaging; DIC image of infected macrophages was merged with Hoechst 33342 nuclei staining channel (blue) and yellow squares that represent the software counting hits. Time of image acquisition is represented by days:hours:minutes: seconds:milliseconds (d:hh:mm:ss:sss). Bar = 30 μm (10 or 15 μm in zoomed region) QuickTime .mov file (H.264 codec).

**Video S3.** Micro-irradiation of host cell nuclei induces cell death and amastigote transfer. Two examples of micro-irradiation experi-

ments (videos A and B) in which macrophage nuclei were micro-irradiated with near UV (405 nm) laser at 400 Hz for 5 min. Video shows micro-irradiated and non-irradiated BMDMØ-GFP in green, *Leishmania amazonensis*-DsRed2 in red and Hoechst 33342 in cyan channel and DIC. Videos are presented in the sequence: (i) micro-irradiation spots visualization in orange, defined by regions of interest (ROI) in which the laser was applied. Micro-irradiated cells are outlined in white, (ii) DIC merged with red and blue channels. Arrowheads indicate amastigote transfers, (iii) green, red and blue channels merged. Amastigotes are transferred with concomitant GFP leakage of the donor host cell. Transferred amastigotes develop spacious parasitophorous vacuoles in recipient macrophages. Time of image acquisition is represented by days:hours:minutes:seconds:milliseconds (d:hh:mm:ss:sss). Image acquisition was started after 72 h (A) or 120 h (B) of infection plus 5 min of micro-irradiation. Bar = 10 μm. QuickTime .mov file (H.264 codec)

**Video S4.** Multidimensional live imaging of micro-irradiated, 48 h infected BMDMØ in the presence of the phosphatidylserine (PS) probe Annexin V (conjugated to CF633 flurophore, cyan) and the cell membrane-impermeant nucleic probe YO-PRO-1 Iodide (yellow). The video shows one infected macrophage in which a concentrated, near-UV laser pulse is applied in the nucleus region (micro-irradiation spot) for 7 min. After this period, multidimensional recordings started: at time point 0d12:53, during macrophage apoptosis (Annexin V-positive, YO-PRO-1-negative staining), *L. amazonensis*-DsRed2 amastigotes (red) are relocated to zeiotic structures which expose PS (arrowhead); the host cell starts necrosis around 0d14:00 (YO-PRO-1 staining is indicative of loss of membrane integrity). Time of image acquisition is represented by days:hours:minutes (d:hh:mm). Bar = 10 μm. QuickTime .mov file (H.264 codec)

**Video S5.** A. BMDMØ-GFP infected with *Leishmania amazonensis*-DsRed2 for 20 days treated with 50 ng $ml^{-1}$ Streptolysin O (SLO), washed from cultures after a pulse of 20 min in phosphate-buffered saline (PBS), observed by multidimensional imaging. The video shows two examples of acquired microscopic fields of an infected culture (out of 10 fields in this experiment). Some host cells lost GFP signal, indicating GFP leakage/loss of membrane integrity; amastigotes contained within these cells were rescued by vicinal, GFP-positive macrophages. Transfers are indicated by arrowheads. Green (BMDMØ-GFP) and red (*L. amazonensis*-DsRed2) fluorescent channels are merged with DIC channel. Time of image acquisition is represented by days:hours:minutes:seconds:milliseconds (d:hh:mm:ss:sss). Bars = 15 μm (first example) and 10 μm (second example). QuickTime .mov file (H.264 codec)

B. BMDMØ-GFP infected with *L. amazonensis*-DsRed2 for 20 days treated with 30 μM nocodazole, maintained in medium, observed by multidimensional imaging. Image acquisition started after 20 days of infection. Treatment with nocodazole induced the formation of blebs containing parasites but not host cell death or cell-to-cell transfer of amastigotes. Green (BMDMØ-GFP) and red (*L. amazonensis*-DsRed2) fluorescent channels are merged with DIC channel. Time of image acquisition is represented by days:hours:minutes:seconds:milliseconds (d:hh:mm:ss:sss). Bar = 10 μm.

**Video S6.** Amastigotes are transferred from cell to cell associated with phagolysosomal components. Video presents multidimensional imaging of RAW 264.7 cells expressing fluorescent lysosome-associated membrane protein-1 (LAMP1, A–B), Rab7 GTPase (C–D) or actin (E) and infected with *Leishmania amazonensis*-DsRed2. Fluorescent channels are merged with DIC image. Image acquisition started after 24 h of infection plus 2 min of micro-irradiation.

A–B. Two examples of RAW 264.7 cells expressing GFP-tagged LAMP1 (green) and infected with *L. amazonensis*-DsRed2 (red). Amastigotes (arrowheads) are transferred associated with a polarized LAMP1-positive cap (A) or fully surrounded by this lysosomal component (B). Time of image acquisition is represented by hours:minutes:seconds:milliseconds (hh:mm:ss:sss). Bars = 10 μm.

C–D. Two examples of RAW 264.7 cells expressing GFP-tagged Rab7 GTPase (green) and infected with *L. amazonensis*-DsRed2 (red). In (C), some amastigotes are extruded in association with Rab7 (arrowhead). Time of image acquisition is represented by days:hours:minutes:seconds:milliseconds (d:hh:mm:ss:sss). Bars = 10 μm. In (D) amastigotes are extruded in Rab7-positive exosomes and transferred (arrowhead) to vicinal macrophages in association with this late endosome marker. Time of image acquisition is represented by hours:minutes:seconds:milliseconds (hh:mm:ss:sss). Bars = 10 μm.

E. Multidimensional imaging of RAW 264.7 cells expressing RFP-tagged actin (shown in green) and infected with *L. amazonensis*-GFP (shown in red). Although extrusions present a transient association with actin, this cytoskeleton component was not transferred to recipient macrophages in association with transferred amastigotes (arrowhead). Time of image acquisition is represented by days:hours:minutes:seconds:milliseconds (d:hh:mm:ss:sss). Bars = 20 μm. QuickTime .mov file (H.264 codec)